

## Understanding Blue-to-Red Conversion in Monomeric Fluorescent Timers and Hydrolytic Degradation of Their Chromophores

Sergei Pletnev,<sup>\*,†,‡</sup> Fedor V. Subach,<sup>§</sup> Zbigniew Dauter,<sup>†</sup> Alexander Wlodawer,<sup>‡</sup> and Vladislav V. Verkhusha<sup>\*,§</sup>

*Synchrotron Radiation Research Section, Macromolecular Crystallography Laboratory, National Cancer Institute, Argonne, Illinois 60439, Basic Research Program, SAIC-Frederick, 9700 South Cass Avenue, Argonne, Illinois 60439, Department of Anatomy and Structural Biology, and Gruss-Lipper Biophotonics Center, Albert Einstein College of Medicine, 1300 Morris Park Avenue, Bronx, New York 10461, and Protein Structure Section, National Cancer Institute at Frederick, Building 536, Frederick, Maryland 21702*

Received October 2, 2009; E-mail: pletnevs@mail.nih.gov; vladislav.verkhusha@einstein.yu.edu

**Abstract:** Fast-FT is a fluorescent timer (FT) engineered from DsRed-like fluorescent protein mCherry. Crystal structures of Fast-FT (chromophore Met66-Tyr67-Gly68) and its precursor with blocked blue-to-red conversion Blue102 (chromophore Leu66-Tyr67-Gly68) have been determined at the resolution of 1.15 Å and 1.81 Å, respectively. Structural data suggest that blue-to-red conversion, taking place in Fast-FT and in related FTs, is associated with the oxidation of  $\alpha 2$ -C $\beta$ 2 bond of Tyr67. Site directed mutagenesis revealed a crucial role of Arg70 and Tyr83 in the delayed oxidation of  $\alpha 2$ -C $\beta$ 2 bond, introducing the timing factor in maturation of the timer. Substitutions Ser217Ala and Ser217Cys in Fast-FT substantially slow down formation of an intermediate blue chromophore but do not affect much blue-to-red conversion, whereas mutations Arg70Lys or Trp83Leu, having little effect on the blue chromophore formation rate, markedly accelerates formation of the red chromophore. The chromophore of FTs adopts a *cis*-conformation stabilized by a hydrogen bond between its phenolate oxygen and the side chain hydroxyl of Ser146. In Blue102, a bulky side chain of Ile146 precludes the chromophore from adopting a “*cis*-like” conformation, blocking its blue-to-red conversion. Both Fast-FT and Blue102 structures revealed hydrolytic degradation of the chromophores. In Fast-FT, chromophore-forming Met66 residue is eliminated from the polypeptide chain, whereas Leu66 in Blue102 is cleaved out from the chromophore, decarboxylated and remains attached to the preceding Phe65. Hydrolysis of the chromophore competes with chromophore maturation and is driven by the same residues that participate in chromophore maturation.

### 1. Introduction

In recent years, fluorescent proteins (FPs) have become invaluable tools in molecular biology.<sup>1,2</sup> Unlike synthetic fluorescent markers, FPs are nontoxic and can be genetically encoded, to be produced by a cell itself. Linking them with protein of interest at the DNA level enables their application as *in vivo* fluorescent markers suitable for visualization of various processes in live cells and tissues in real time. Since their discovery, natural FPs found in marine organisms have been substantially improved in brightness, color palette, and photostability; a wide range of methods using FPs have been

designed to study intracellular molecules,<sup>3</sup> gene activities,<sup>4</sup> relative age of organelles,<sup>5</sup> and cell differentiation.<sup>6</sup> A great effort has been put into developing specialized FP-biomarkers such as photoactivatable FPs,<sup>7</sup> pH-,<sup>8</sup> redox-,<sup>9</sup> and ion (Ca<sup>2+</sup>) sensors.<sup>10</sup> A group of FPs capable of changing color over a specific period of time was one of such specialty probes. They were named fluorescent timers (FTs)<sup>6</sup> and quickly became

<sup>†</sup> Synchrotron Radiation Research Section, Macromolecular Crystallography Laboratory, National Cancer Institute.

<sup>‡</sup> Basic Research Program, SAIC-Frederick.

<sup>§</sup> Department of Anatomy and Structural Biology, and Gruss-Lipper Biophotonics Center, Albert Einstein College of Medicine.

<sup>‡</sup> National Cancer Institute at Frederick.

(1) Chudakov, D. M.; Lukyanov, S.; Lukyanov, K. A. *Trends Biotechnol.* **2005**, *23* (12), 605–613.

(2) Stepanenko, O. V.; Verkhusha, V. V.; Kuznetsova, I. M.; Uversky, V. N.; Turoverov, K. K. *Curr. Protein Pept. Sci.* **2008**, *9* (4), 338–369.

(3) Shaner, N. C.; Patterson, G. H.; Davidson, M. W. *J. Cell Sci.* **2007**, *120* (Pt 24), 4247–4260.

(4) Mirabella, R.; Franken, C.; van der Krogt, G. N.; Bisseling, T.; Geurts, R. *Plant Physiol* **2004**, *135* (4), 1879–1887.

(5) Duncan, R. R.; Greaves, J.; Wiegand, U. K.; Matskevich, I.; Bodamer, G.; Apps, D. K.; Shipston, M. J.; Chow, R. H. *Nature* **2003**, *422* (6928), 176–180.

(6) Terskikh, A.; Fradkov, A.; Ermakova, G.; Zarskiy, A.; Tan, P.; Kajava, A. V.; Zhao, X.; Lukyanov, S.; Matz, M.; Kim, S.; Weissman, I.; Siebert, P. *Science* **2000**, *290* (5496), 1585–1588.

(7) Lukyanov, K. A.; Chudakov, D. M.; Lukyanov, S.; Verkhusha, V. V. *Nat. Rev. Mol. Cell Biol.* **2005**, *6* (11), 885–891.

(8) Miesenbock, G.; De Angelis, D. A.; Rothman, J. E. *Nature* **1998**, *394* (6689), 192–195.

(9) Ostergaard, H.; Henriksen, A.; Hansen, F. G.; Winther, J. R. *EMBO J.* **2001**, *20* (21), 5853–5862.

(10) Miyawaki, A.; Griesbeck, O.; Heim, R.; Tsien, R. Y. *Proc. Natl. Acad. Sci. U.S.A.* **1999**, *96* (5), 2135–2140.

indispensable molecular tools for using when an accurate insight into the timing of intracellular processes needs to be established. Until the end of 2008, the only FT generally available to the scientific community was DsRed-E5.<sup>6</sup> It proved to be highly successful in the studies of promoter activity,<sup>6</sup> but the tetrameric nature of this biomarker limited its application for protein tagging. Recently, a new series of monomeric FTs consisting of three mCherry-derived variants exhibiting a distinct fast, medium, and slow blue-to-red chromophore transitions has been developed.<sup>11</sup>

A typical FP is a globular protein in the form of a  $\beta$ -barrel, with an embedded chromophore unit in its center. Such an architecture isolates the chromophore moiety from the exterior, eliminating quenching of the fluorophore by water, and thus is essential for supporting the fluorescent properties of FP. The chromophore is formed spontaneously in the course of post-translational chemical reactions after protein folding is complete.<sup>12</sup> There are no known cofactors or enzymatic components required for this apparently autocatalytic process that involves catalysis by specific amino acid residues present in all FPs. In some cases, posttranslational modification leads solely to chromophore formation, whereas in other cases, the same residues could catalyze chromophore degradation, seen as FP fading, discoloration, or color change. The fluorescent properties, mechanism of chromophore formation, and stability of FP depend on the protein structure and, in particular, on the amino acid residues forming the chromophore and those in its immediate vicinity.

Starting from the discovery of *Aequorea victoria* green fluorescent protein (*avGFP*), numerous studies have been aimed at establishing the mechanism of chromophore formation. Finally, it was shown that in different marine organisms the formation of cyan and green chromophores in FPs follows an identical path of the polypeptide backbone cyclization with subsequent oxidation of the C $\alpha$ 2–C $\beta$ 2 bond of the second chromophore-forming residue.<sup>13,14</sup> The resulting structures have a bicyclic core identical to that of *avGFP*.<sup>15</sup> Regarding the driving force of chromophore formation, mechanical compression hypothesis suggests that peptide cyclization is caused by a tendency to relax an energetically unfavorable precyclized state.<sup>16</sup> Yellow and red FPs undergo an additional sequence of transformations resulting in formation of tricyclic structures<sup>14,17–19</sup> or bicyclic structures with an acylimine bond between the chromophore and the preceding polypeptide residue.<sup>20–26</sup> Such

extension of the conjugated system of the chromophore causes a bathochromic shift of its emission band.

In the most optimized fluorescent proteins, chromophore maturation happens within a couple of hours after protein folding,<sup>1,2</sup> whereas in FTs this process is substantially extended in time. In order to shed light on the events taking place in the course of FTs clocking time, we have crystallized and solved the structures of Fast-FT derived from mCherry in the FT's final clocking point, red form, as well as of its blue precursor, Blue102, with the maturation blocked in the initial clocking point of FTs, in a blue form. We then analyzed the environments of their chromophores, produced test mutants, and examined their spectral properties and kinetics of maturation. This study allowed us to reveal key residues assisting chromophore maturation, to understand the mechanism of blue-to-red conversion, and to discover how to alter the kinetics of posttranslational reactions in FTs. The results extend our knowledge of post-translational chemistry in FPs and can help in creating novel biomarkers with time-resolved properties.

## 2. Experimental Procedures

**2.1. Mutagenesis, Expression, and Purification.** Site-specific mutagenesis of the genes encoding Fast-FT, Blue102, and Blue124 in pBAD/HisB vector (Invitrogen) was performed using the QuickChange mutagenesis kit (Stratagene), according to the manufacturer's protocol.

For crystallization and spectroscopic measurements the recombinant fluorescent proteins with the N-terminal His<sub>6</sub>-tag were expressed in the LMG194 bacterial strain (Invitrogen) by overnight culture in RM minimal medium at 37 °C in the presence of 0.004% arabinose. The culture was then centrifuged at 5000 rpm at 4 °C for 15 min, and the cell pellet was resuspended in 50 mM NaH<sub>2</sub>PO<sub>4</sub>, 300 mM NaCl, pH 8.0 buffer and lysed by sonication on ice.

The recombinant proteins were further purified with Ni-NTA resin (Qiagen) followed by size exclusion chromatography on Superdex 200 column (GE-HealthCare) in 20 mM Tris-HCl pH 8.0, 200 mM NaCl, and 5 mM EDTA. Buffer exchange and protein concentration were performed in VivaSpin 15 MWCO 10 kDa sample concentrators (VivaScience). Protein stock for crystallization contained 45.0 mg/mL of each protein in 10 mM Tris-HCl pH 8.0, 100 mM NaCl, and 2.5 mM EDTA.

**2.2. Proteins for Spectroscopic and Timing Properties.** To purify proteins for maturation kinetic measurements, LMG194 cells grown overnight were diluted to an optical density of 1.0 at 600 nm, and 0.2% arabinose was added for induction of protein expression. The bacterial cultures were then grown at 37 °C in completely filled 50 mL tubes tightly sealed to restrict oxygen supply. After 1 h, the cultures were pelleted down in the same tightly closed tubes. After opening the tubes, the proteins were purified using B-Per reagent (Pierce) and Ni-NTA resin (Qiagen) within 30 min, with all procedures conducted at 4 °C to inhibit chromophore maturation. The purified proteins were either im-

- (11) Subach, F. V.; Subach, O. M.; Gundorov, I. S.; Morozova, K. S.; Piatkevich, K. D.; Cuervo, A. M.; Verkhusha, V. V. *Nat. Chem. Biol.* **2009**, *5* (2), 118–126.
- (12) Barondeau, D. P.; Putnam, C. D.; Kassmann, C. J.; Tainer, J. A.; Getzoff, E. D. *Proc. Natl. Acad. Sci. U.S.A.* **2003**, *100* (21), 12111–12116.
- (13) Henderson, J. N.; Remington, S. J. *Proc. Natl. Acad. Sci. U.S.A.* **2005**, *102* (36), 12712–12717.
- (14) Remington, S. J.; Wachter, R. M.; Yarbrough, D. K.; Branchaud, B.; Anderson, D. C.; Kallio, K.; Lukyanov, K. A. *Biochemistry* **2005**, *44* (1), 202–212.
- (15) Ormo, M.; Cubitt, A. B.; Kallio, K.; Gross, L. A.; Tsien, R. Y.; Remington, S. J. *Science* **1996**, *273* (5280), 1392–1395.
- (16) Baedeker, M.; Schulz, G. E. *Structure* **2002**, *10* (1), 61–67.
- (17) Pletneva, N. V.; Pletnev, S. V.; Chudakov, D. M.; Tikhonova, T. V.; Popov, V. O.; Martynov, V. I.; Wlodawer, A.; Dauter, Z.; Pletnev, V. Z. *Bioorg. Khim.* **2007**, *33* (4), 421–430.
- (18) Shu, X.; Shaner, N. C.; Yarbrough, C. A.; Tsien, R. Y.; Remington, S. J. *Biochemistry* **2006**, *45* (32), 9639–9647.
- (19) Mizuno, H.; Mal, T. K.; Tong, K. I.; Ando, R.; Furuta, T.; Ikura, M.; Miyawaki, A. *Mol. Cell* **2003**, *12* (4), 1051–1058.
- (20) Baird, G. S.; Zacharias, D. A.; Tsien, R. Y. *Proc. Natl. Acad. Sci. U.S.A.* **2000**, *97* (22), 11984–11989.

- (21) Gross, L. A.; Baird, G. S.; Hoffman, R. C.; Baldrige, K. K.; Tsien, R. Y. *Proc. Natl. Acad. Sci. U.S.A.* **2000**, *97* (22), 11990–11995.
- (22) Yarbrough, D.; Wachter, R. M.; Kallio, K.; Matz, M. V.; Remington, S. J. *Proc. Natl. Acad. Sci. U.S.A.* **2001**, *98* (2), 462–467.
- (23) Wall, M. A.; Socolich, M.; Ranganathan, R. *Nat. Struct. Biol.* **2000**, *7* (12), 1133–1138.
- (24) Petersen, J.; Wilmann, P. G.; Beddoe, T.; Oakley, A. J.; Devenish, R. J.; Prescott, M.; Rossjohn, J. *J. Biol. Chem.* **2003**, *278* (45), 44626–44631.
- (25) Pletnev, S.; Shcherbo, D.; Chudakov, D. M.; Pletneva, N.; Merzlyak, E. M.; Wlodawer, A.; Dauter, Z.; Pletnev, V. *J. Biol. Chem.* **2008**, *283* (43), 28980–28987.
- (26) Pletneva, N.; Pletnev, V.; Tikhonova, T.; Pakhomov, A. A.; Popov, V.; Martynov, V. I.; Wlodawer, A.; Dauter, Z.; Pletnev, S. *Acta Crystallogr., Sect. D.* **2007**, *63* (Pt 10), 1082–1093.

**Table 1.** Data Collection Statistics<sup>a</sup>

protein	Fast-FT	Blue102
space group	<i>P</i> 2 <sub>1</sub>	<i>C</i> 2
unit cell parameters (Å, deg)	<i>a</i> = 48.8 <i>b</i> = 42.5 <i>c</i> = 61.8 $\beta$ = 112.1	<i>a</i> = 107.4 <i>b</i> = 42.3 <i>c</i> = 85.0 $\beta$ = 127.1
temperature (K)	100	100
wavelength (Å)	1.00	1.00
resolution (Å)	30.0–1.15	30.0–1.81
total reflections	296,096	111,099
unique reflections	83,298	27,667
completeness (%)	99.7 (97.3)	98.1 (85.8)
<i>I</i> / $\sigma$ ( <i>I</i> )	22.5 (2.2)	19.3 (2.4)
<i>R</i> -merge	0.048 (0.457)	0.063 (0.418)
multiplicity	3.6 (2.7)	4.0 (3.2)

<sup>a</sup>Data in parentheses are for the outermost resolution shells, 1.19–1.15 Å for Fast-FT, and 1.87–1.81 Å for Blue102.

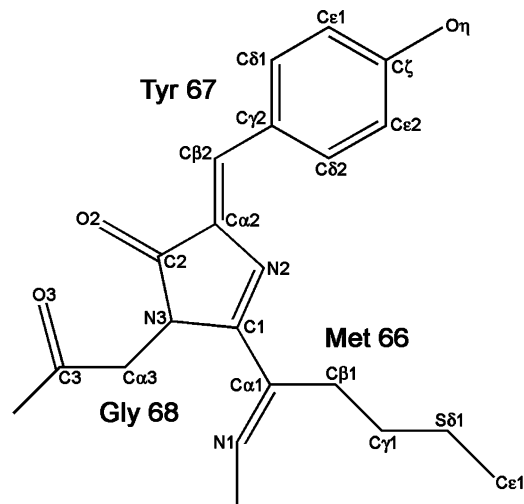
mediately frozen in liquid nitrogen or applied to kinetic measurements at 37 °C.

Absorbance spectra were recorded on the U-3010 spectrophotometer (Hitachi). The excitation and emission spectra were measured using the FluoroMax-3 spectrofluorometer (Horiba Jobin Yvon). All spectral measurements were performed with the protein samples in phosphate-buffered saline (PBS). Protein concentrations were determined using the BCA assay (Pierce).

**2.3. Crystallization and Data Collection.** The crystals of Fast-FT were obtained by hanging drop vapor diffusion from 1  $\mu$ L of protein mixed with 1  $\mu$ L of the well solution (0.2 M MgCl<sub>2</sub> × 6H<sub>2</sub>O, 0.1 M Tris-HCl pH 8.5, 30% w/v PEG4000) incubated against 500  $\mu$ L of the same reservoir at 20 °C for 2 weeks. Blue102 was crystallized by the same method from 0.1 M citric acid pH 5.0, 1.0 M LiCl, 20% w/v PEG6000. The growth time for Blue102 crystals was about 2 weeks. An extensive search for crystallization conditions for Blue124 did not result in any successful hits.

X-ray diffraction data for both Fast-FT and Blue102 were collected at the Advanced Photon Source, SER-CAT beamline 22-ID (Argonne National Laboratory, Argonne, IL). Diffraction intensities were registered on a MAR300 CCD detector (MAR Research). Prior to data acquisition a single crystal was dipped into cryoprotecting solution composed of 20% (v/v) of glycerol and 80% (v/v) of the corresponding well solution and flash cooled in 100 K nitrogen stream. Cryogenic temperature was maintained throughout the diffraction experiment with an Oxford Cryostream cooling device (Oxford Cryosystems). Diffraction images were indexed, integrated, and scaled with HKL2000.<sup>27</sup> The statistics of data processing is shown in Table 1.

**2.4. Structure Solution and Refinement.** The structures of Fast-FT and Blue102 were solved by molecular replacement method with *MOLREP*<sup>28</sup> using a monomer of mCherry (PDB ID 2H5Q)<sup>18</sup> without its chromophore moiety as the search model. Maximum likelihood refinement and real space model correction were performed with *PHENIX*<sup>29</sup> and *COOT*,<sup>30</sup> respectively. Ordered water molecules were added to the appropriate difference electron density peaks with *COOT* and *PHENIX*. Structure quality was validated with *PROCHECK*<sup>31</sup> and *COOT*. The refinement statistics

**Figure 1.** Chemical structure of Fast-FT chromophore.**Table 2.** Refinement Statistics

	Fast-FT	Blue102
no. of protein atoms	2024	1890
no. of solvent atoms	394	278
resolution range (Å)	30.0–1.15	30.0–1.81
<i>R</i> <sub>work</sub>	0.149	0.213
<i>R</i> <sub>free</sub>	0.177	0.256
rmsd bond lengths (Å)	0.011	0.013
rmsd angles (deg)	1.54	1.57
rmsd chirality (deg)	0.10	0.11
rmsd planarity (deg)	0.009	0.006
rmsd dihedral (deg)	15.8	17.2
Mean <i>B</i> Factors (Å <sup>2</sup> ) Protein Atoms		
overall	12.6	26.8
main chain	10.8	24.5
side chain	14.3	29.1
Ramachandran Statistics (%) (for non-Gly/Pro Residues)		
most favorable	95.6	95.7
additionally allowed	4.4	4.3

are summarized in Table 2. The coordinates and structure factors were deposited in the Protein Data Bank and assigned accession codes 3LF3 and 3LF4 for Fast-FT and Blue102, respectively.

### 3. Results

**3.1. Properties of Fast-FT, Blue102, and Blue124.** Fast-FT is a fluorescent timer engineered from mCherry, a DsRed-like fluorescent protein.<sup>11</sup> It contains a DsRed-like chromophore moiety (Figure 1) and is characterized by pronounced delay in chromophore formation. Maturation of Fast-FT manifests itself in the protein absorbance spectra as an increase of intensity of its 403 nm band that, at 37 °C, reaches a maximum in 15 min after the protein folding is complete. The following slow blue-to-red conversion appears as a decrease of the blue band intensity and a simultaneous growth of the red band, with a maximum at 583 nm. The blue band completely disappears in 16 h, while the red one reaches its maximum intensity in about 24 h, marking the end of the blue-to-red conversion.<sup>11</sup> While screening for Fast-FT, we found several precursor variants with blue-to-red conversion blocked in the blue state, including Blue102 and Blue124 (Figure 2). Maturation of purified Blue102 and Blue124 ends at the blue-emitting form corresponding to the maximum intensity of the 403 nm absorbance band. The

(27) Otwinowski, Z.; Minor, W. *Methods Enzymol.* **1997**, *276*, 307–326.

(28) Vagin, A.; Teplyakov, A. *Acta Crystallogr., Sect. D.* **2000**, *56* (Pt 12), 1622–1624.

(29) Adams, P. D.; Grosse-Kunstleve, R. W.; Hung, L. W.; Ioerger, T. R.; McCoy, A. J.; Moriarty, N. W.; Read, R. J.; Sacchettini, J. C.; Sauter, N. K.; Terwilliger, T. C. *Acta Crystallogr., Sect. D* **2002**, *58* (Pt 11), 1948–1954.

(30) Emsley, P.; Cowtan, K. *Acta Crystallogr., Sect. D* **2004**, *60* (Pts 12, 1), 2126–2132.

(31) Laskowski, R. A.; Rullmann, J. A.; MacArthur, M. W.; Kaptein, R.; Thornton, J. M. *J. Biomol. NMR* **1996**, *8* (4), 477–486.

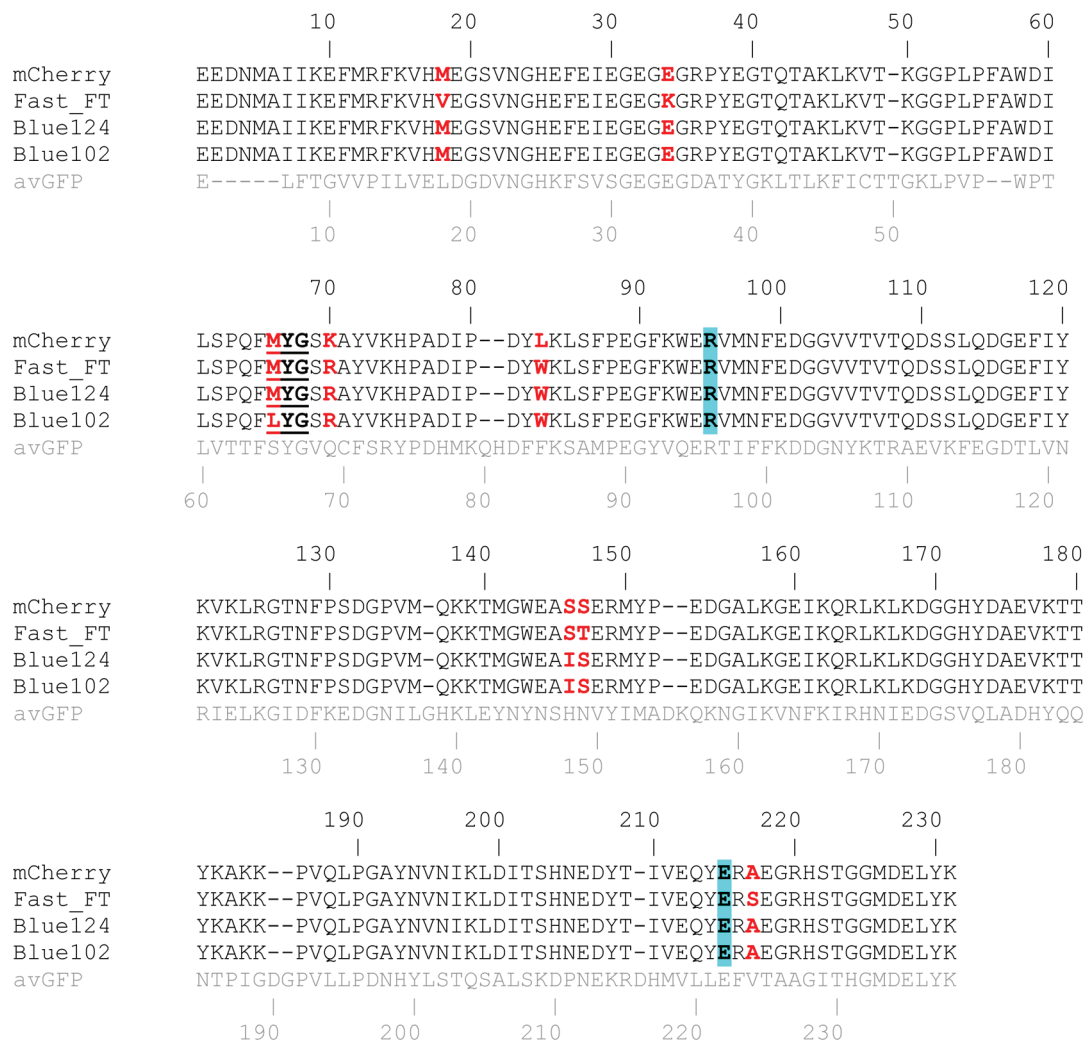


**Figure 2.** Amino acid sequence alignment of mCherry, Fast-FT, Blue124, Blue102, and *Aequorea victoria* GFP (in gray). Differences between the residues are indicated in red. Chromophore-forming residues are underlined. Catalytic Arg95 and Glu215 are highlighted in blue. Numbering above (in black) and below (in gray) correspond to mCherry and to avGFP, respectively.

sequence of chemical transformations occurring in the course of posttranslational events in Fast-FT, Blue102, and Blue124 will be discussed in detail below.

**3.2. Crystal Structures.** We have determined the crystal structures of Fast-FT and its precursor, Blue102, at 1.15 Å and 1.81 Å resolution, respectively (Table 2). The non-isomorphous asymmetric units of the crystals of both proteins contain one monomer each. Space group symmetry operators do not generate tetramers or dimers for either Fast-FT or Blue102, indicating a monomeric state of both proteins. No electron density was observed for the N-terminal His-tags as well as for residues 1–4 and 225–231 of Fast-FT, and 1–4 and 228–231 of Blue102, indicating their disorder. As seen in the electron density maps, the loop region 163–173 in Blue102 is able to adopt multiple conformations of the polypeptide chain. However, this stretch of residues is well ordered and invariant in Fast-FT. Multiple conformations of the side chains were observed for 25 (10.8%) residues of Fast-FT and 11 (4.8%) residues of Blue102. Structure validation revealed that 95.6% of residues in Fast-FT and 95.7% of residues in Blue102 are grouped in the most favored regions of the Ramachandran plot, and the remaining residues are located in the additional allowed regions, indicating no significant departure from nonstrained geometry. Superposition of C $\alpha$  atoms of Fast-FT and Blue102 on mCherry

yielded the corresponding root-mean-square deviations of 0.25 Å and 0.34 Å, respectively, demonstrating the similarity of the tertiary structures of these proteins.

**3.3. Structural Differences and Similarities of Fast-FT, Blue102, and mCherry.** The primary structure of Fast-FT differs from its progenitor mCherry by replacement of six amino acid residues (Figure 2): Met18Val, Glu34Lys, Lys70Arg, Leu83Trp, Ser147Thr, and Ala217Ser. Two of them, Lys34 and Thr147, are located on the surface of the protein globule; Arg70 and Ser217 are part of the immediate chromophore environment, whereas Val18 and Trp83 belong to the second shell of residues surrounding the chromophore moiety (Figure 3).

Surface residues 34 and 147 are located on the opposite sides of the  $\beta$ -barrel with respect to each other. Lys34 in Fast-FT forms a hydrogen bond with the Glu30 of a symmetry-related molecule (N $\zeta$ –O $\epsilon$ 1 2.73 Å), whereas Glu34 of mCherry, having a shorter side chain, does not interact with the adjacent monomer. Residue 147 (threonine in Fast-FT and serine in mCherry) lies in the vicinity of the hydroxyl of the phenolic ring of the chromophore, but interacts neither with the latter nor with any symmetry-related molecules and is exposed to solvent. Residue 18 belongs to the second shell of the residues surrounding the chromophore and is separated from the moiety by Gln64. This position is occupied by valine in Fast-FT and

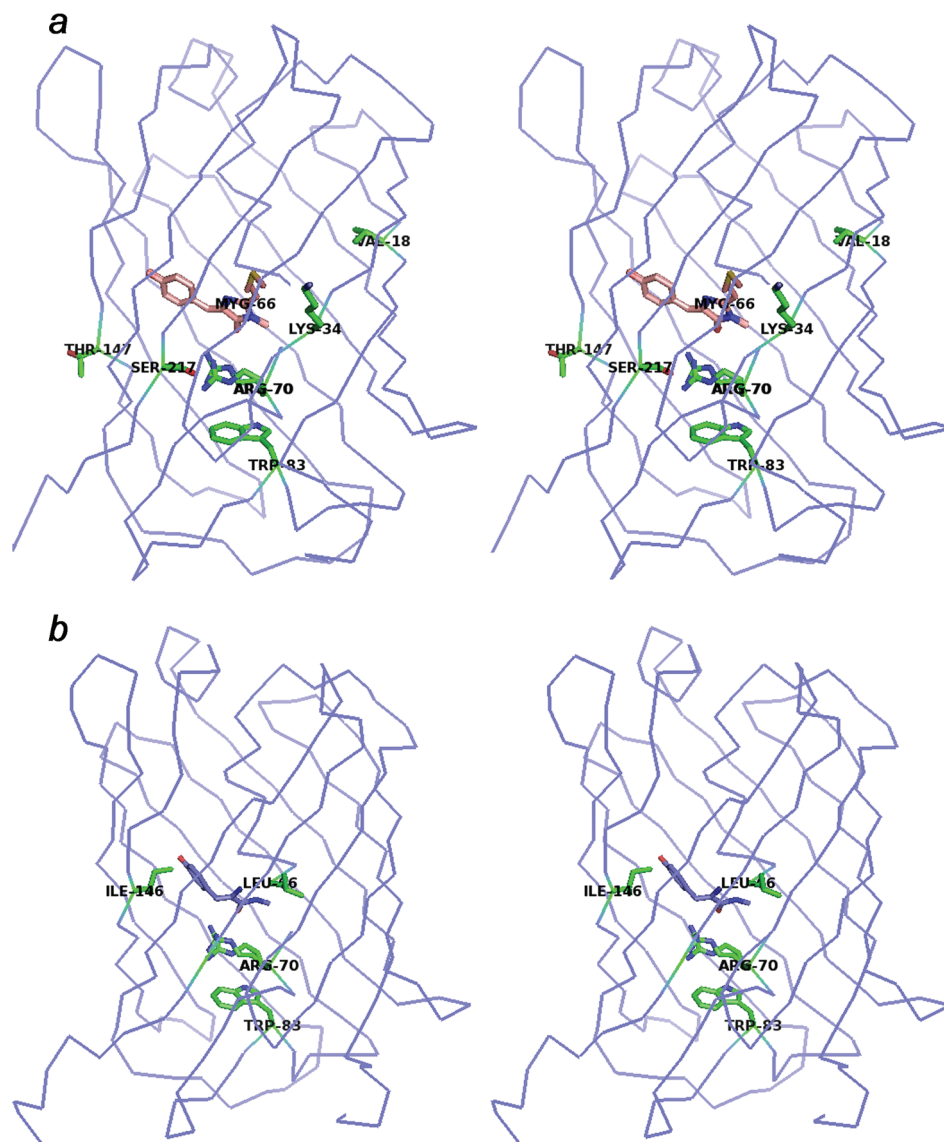


**Figure 3.** Stereo representation of the residues that differ between (a) Fast-FT and mCherry and (b) Blue102 and mCherry. Fast-FT and Blue102 chromophores are shown in pink and blue, respectively; residues of Fast-FT and Blue102 that differ from those in mCherry are shown in green.

by methionine in mCherry, and this residue faces a hydrophobic pocket formed by Phe27, Ile29, Leu61, Phe65, Val122, and Leu124.

Two very important residues, Arg70 and Trp83 in Fast-FT and their counterparts Lys70 and Leu83 in mCherry, deserve special attention. Arg70 is located at the side of the chromophore, in its immediate vicinity. Its guanidine group resides within 3.70–4.46 Å from the C $\alpha$ 2 and C $\beta$ 2 atoms and within 3.1 Å from the imidazolone carbonyl of the chromophore (Figure 4a). Arg70 is observed in two alternative conformations, each with occupancy of 0.5. In conformation “A”, the guanidine group of Arg70 forms hydrogen bonds with the carboxyl of Glu148 (N $\eta$ 1–O $\epsilon$ 1 2.56 Å, N $\eta$ 2–O $\epsilon$ 1 2.60 Å) and the carbonyl of the chromophore imidazolone ring (N $\epsilon$ –O2 3.08 Å). Conformation “B” retains a similar hydrogen bond pattern with Glu148 (N $\eta$ 1–O $\epsilon$ 1 2.99 Å, N $\eta$ 2–O $\epsilon$ 1 2.80 Å), but instead of a hydrogen bond between N $\epsilon$  of Arg70 and O2 of the chromophore, it forms one between N $\eta$ 1 of Arg70 and O2 (N $\eta$ 1–O2 3.13 Å). From the side opposite to the chromophore, Arg70 is flanked by the side chain of Trp83. Its indole ring is positioned at a  $\sim$ 60° angle relative to the plane of the

guanidinium group of Arg70 and at about 4 Å distance from the arginine. Lys70 of mCherry is located within the same  $\sim$ 4.0 Å distance from the chromophore, yet it is not hydrogen bonded to it. At the side opposite from the chromophore, Lys70 is not supported by any other residue, since a much smaller Leu83 is located too far to establish any significant contacts with the lysine. The only hydrogen bond formed by Lys70 is between its amine nitrogen and the carboxyl oxygen of Glu148 (N $\epsilon$ –O $\epsilon$ 1 2.61 Å).

Residue 217 is the last, but not the least important, of the residues distinguishing Fast-FT from mCherry. Ser217 of Fast-FT forms hydrogen bonds with the catalytic Glu215 via a water molecule (Ser217–O $\gamma$ –W128 2.81 Å, W128–Glu215–O $\epsilon$ 2 2.89 Å) (Figure 4a), whereas a residue found in the equivalent position in mCherry is Ala217, not capable of any interactions with Glu215. It is important to note that the conserved catalytic Glu215’s in Fast-FT and mCherry have different conformations. The carboxyl groups of these residues are turned 72.5° with respect to each other ( $\chi$ 3 9.6° and  $-62.9^\circ$  in Fast-FT and mCherry, respectively). Nevertheless, in both Fast-FT and mCherry Glu215 forms strong hydrogen bonds with the imi-

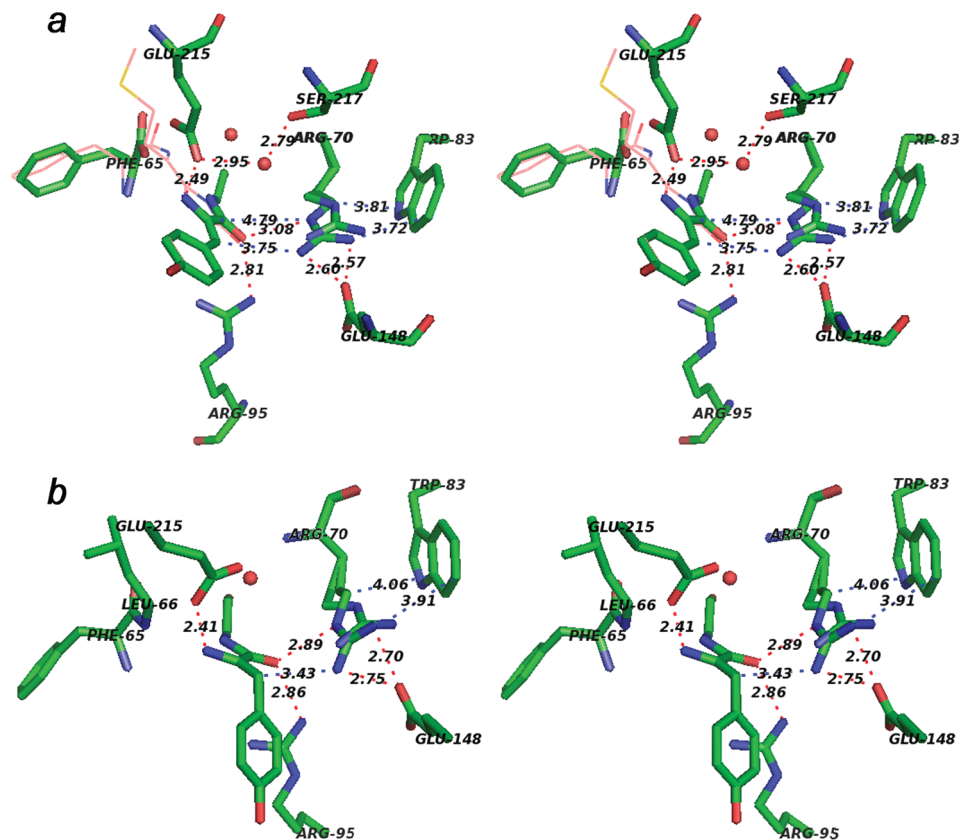


**Figure 4.** Stereo representation of the chromophore environment in Fast-FT and Blue102. (a) A view of the Fast-FT chromophore from the side of its phenolic ring. A degraded chromophore moiety and the preceding Phe65 (occupancies 0.77) are shown in green. An intact red-emitting chromophore and an alternative conformation of Phe65 (occupancies 0.23) are shown in pink. Hydrogen bonds and important close contacts are shown in red and blue dashed lines, respectively. (b) A similar view of the Blue102 chromophore. A degraded nonfluorescent chromophore moiety, decarboxylated Leu66, Phe65, and the important residues of the chromophore environment are shown in green. Hydrogen bonds and important close contacts are shown in red and blue dashed lines, respectively.

dazolone nitrogens of the chromophores ( $O\epsilon 2-N2$  2.49 Å in Fast-FT and  $O\epsilon 1-N2$  2.65 Å in mCherry).

Despite numerous differences between Fast-FT and mCherry, these two FPs retain many identical features. The second conserved catalytic residue, R95, adopts the same conformation in both proteins and forms hydrogen bonds with the imidazolone carbonyl of the chromophore ( $N\eta 2-O2$  2.81 Å). The same is true for Ser146 that forms a stabilizing hydrogen bond with the phenolate  $O\eta$  of the chromophore, favoring the *cis* conformation of the moiety ( $O\gamma-O\eta$  2.71 Å).

The sequence of Blue102 could be considered as an intermediate between mCherry and Fast-FT. It differs from Fast-FT in the identity of six amino acids (Met18, Glu34, Leu66, Ile146, Ser147, and Ala217), whereas only four amino acids (Leu66, Arg70, Trp83, and Ile146) are different compared to mCherry (Figures 2, 3a). Amino acids Met18, Glu34, Ser147, and Ala217 of Blue102 are the same as in mCherry, whereas amino acids Arg70 and Trp83 are the same as in Fast-FT. It is important to note that in Blue102 residues Met18, Glu34, Glu215, and Ala217 adopt the same conformation and have similar contacts with the surrounding residues as those in mCherry, whereas Arg70 and Trp83 maintain interactions with the surrounding residues and the chromophore similar to those in Fast-FT (Figure 4b).

Only two positions, Leu66 and Ile146, distinguish Blue102 from both mCherry and Fast-FT. Unfortunately, the position and conformation of Leu66 in an intact chromophore of Blue102 are unknown, since the crystal structure revealed the presence

of a degraded chromophore moiety (see below). Ile146, on the other hand, partially fills the cavity occupied in Fast-FT and mCherry by the phenolic ring of the chromophore, preventing the chromophore moiety from adopting a *cis* conformation.

**3.4. Unusual Chromophore Degradation.** The chromophore of Fast-FT undergoes an unusual degradation, resulting in complete elimination from polypeptide chain of Met66, the first chromophore-forming residue, introducing a break in the protein backbone between Phe65 and the chromophore (Figure 5a). The electron density indicates the formation of either a carboxyl or an amide at the C terminus of residue 65. Refinement of the structure with the phenylalanine amide (NFA) at position 65 gave closer values of B-factors for N and O atoms than for two carboxyl oxygens of a Phe, suggesting an amide terminus of residue 65. The degraded chromophore moiety of Fast-FT has coplanar disposition of the phenolate and the remnant imidazolone groups, and absorbs at 320 nm. The electron density also features an intact chromophore moiety with the estimated occupancy of 0.23 (Figure 5a); the remaining ~77% of the mature Fast-FT molecules experience chromophore degradation. The phenolic rings of both the degraded and intact chromophores adopt *cis* conformation coplanar with the imidazolone group. The observed *cis* orientation of the chromophore is stabilized by a strong (2.67 Å) hydrogen bond between the side chain hydroxyl of Ser146 and the phenolic ring oxygen of the chromophore.

The chromophore of Blue102 undergoes similar degradation. However, no traces of electron density corresponding to an intact

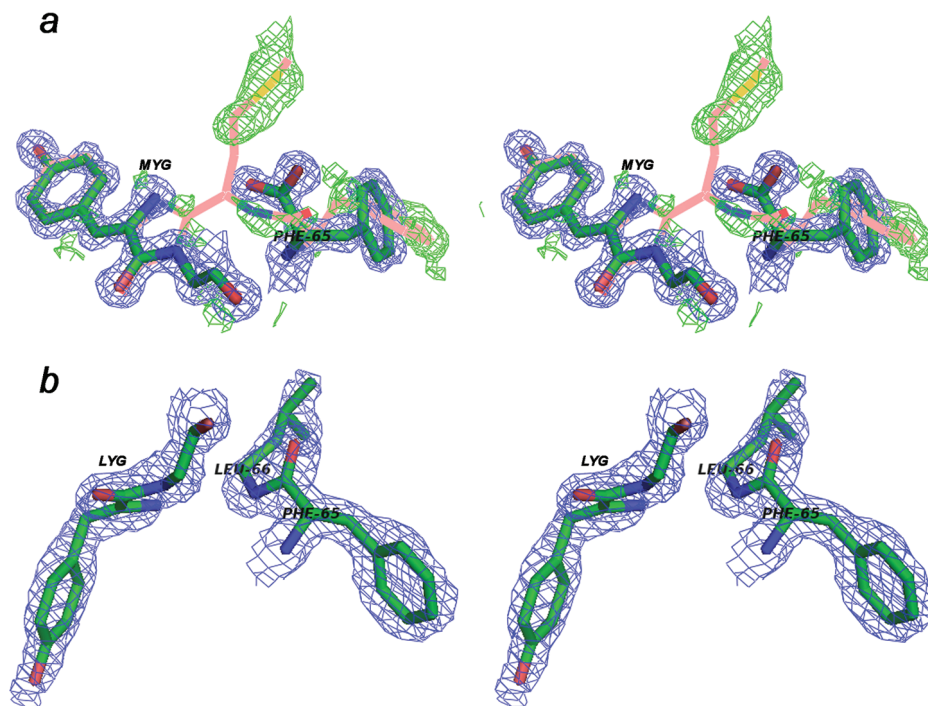


**Figure 5.** (a) Stereo representation of the intact and degraded Fast-FT chromophore moieties in their electron density. The density was calculated in the presence of degraded chromophore moiety and the preceding Phe65 in major conformation, and in the absence of intact chromophore and the preceding Phe65 in minor conformation. Blue:  $2F_o - F_c$  electron density contoured at  $2.0\sigma$  level corresponding to the degraded chromophore and Phe65 in the major conformation (model shown in green). Green: difference  $F_o - F_c$  electron density contoured at  $2.0\sigma$  level corresponding to the intact chromophore and Phe65 in the minor conformation (model shown in pink). (b) Stereo representation of a hydrolyzed Blue102 chromophore moiety, decarboxylated Leu66, and preceding Phe65 in a  $2F_o - F_c$  electron density contoured at  $1.5\sigma$  level.

chromophore were observed, pointing to almost complete decomposition of the chromophore (Figure 5b). Similarly to that of the Fast-FT, the process was accompanied by the cleavage of the 5-membered imidazolone ring and by fragmentation of the peptide bond. Nevertheless Leu66 is not completely eliminated from the protein in Blue102, but only decarboxylated and remaining covalently bound to the preceding Phe65 (Figure 5b). The phenolic ring of the degraded Blue102 chromophore is oriented almost perpendicularly to the remnant imidazolone group, with the torsion angle  $N2-C\alpha2-C\beta2-C\gamma2$  (tilt) of  $90.2^\circ$ . The valence angle  $C\alpha2-C\beta2-C\gamma2$  ( $119.3^\circ$ ) is unusually acute for a typical chromophore moiety ( $134.3^\circ$  in mCherry,<sup>18</sup>  $133.2^\circ$  in Fast-FT, and  $130.5^\circ$  in DsRed<sup>22</sup>), suggesting  $sp^3$ -hybridization of the  $C\beta2$  atom. A degraded chromophore moiety of Blue102 does not have any conjugated  $\pi$ -electron system and therefore cannot emit light, which is consistent with the emission spectra recorded for Blue102 crystals showing no fluorescence at all (data not shown).

**3.5. Mutagenesis.** To assess the importance of the individual residues that differ between Fast-FT and mCherry and which might be responsible for the timing properties of the former protein, we generated five mutants, changing the residues of Fast-FT, one at a time, back to the original mCherry sequence, and examined their spectral properties and kinetics of maturation (Figure 6, Table 3, and Table 1s and Figure 1s of Supporting Information). We also created and characterized three additional mutants of mCherry, Blue102, and Blue124, in which we adjusted single residues to the sequence of Fast-FT.

Reversion of Arg70 back to lysine (Fast-FT/R70K) resulted in a faster maturing FT; formation of its blue and red forms is 3.1-fold and 10.8-fold faster than in original Fast-FT purified protein, respectively. Additionally, the absorbance spectra of this variant show 4.6-fold increase of the 583 nm absorbance

**Table 3.** Spectroscopic and Kinetic Properties of Fast-FT, Blue Precursors, and Mutants

protein		absorbance maximum, nm	$\frac{[A_{Mutant}^{403}/A_{Fast-FT}^{403}]}{[A_{Mutant}^{583}/A_{Fast-FT}^{583}]}$	characteristic times at 37 °C, <sup>a</sup> h
Fast-FT	blue form	403	1.0	0.25
	red form	583	1.0	7.1
Fast-FT/S217C	blue form	403	1.20	2.3
	red form	580	3.01	16.3
Fast-FT/S146A	blue form	403	0.90	0.34
	red form	586	0.12	5.2
Fast-FT/R70K	blue form	403	0.31	0.08
	red form	582	4.64	0.66
Fast-FT/S217A	blue form	403	0.79	1.0
	red form	581	4.27	9.4
Fast-FT/W83L	blue form	410	0.24	0.08
	red form	585	0.18	2.1
Blue 124/I146S	blue form	403	1.21	0.33
	red form	581	5.0	7.4
Blue 102	blue form	403	0.62	0.66
	red form	—	—	—
Blue 124	blue form	403	1.03	2.0
	red form	—	—	—

<sup>a</sup> Characteristic times of Fast-FT, its mutants, and Blue124/I146S correspond to the maxima for the blue forms and to maturation half-times for the red forms. Characteristic times for Blue102 and Blue124 correspond to maturation half-times for their blue forms.

band intensity relative to that of Fast-FT, indicating an increased efficiency of the blue-to-red conversion. An opposite substitution

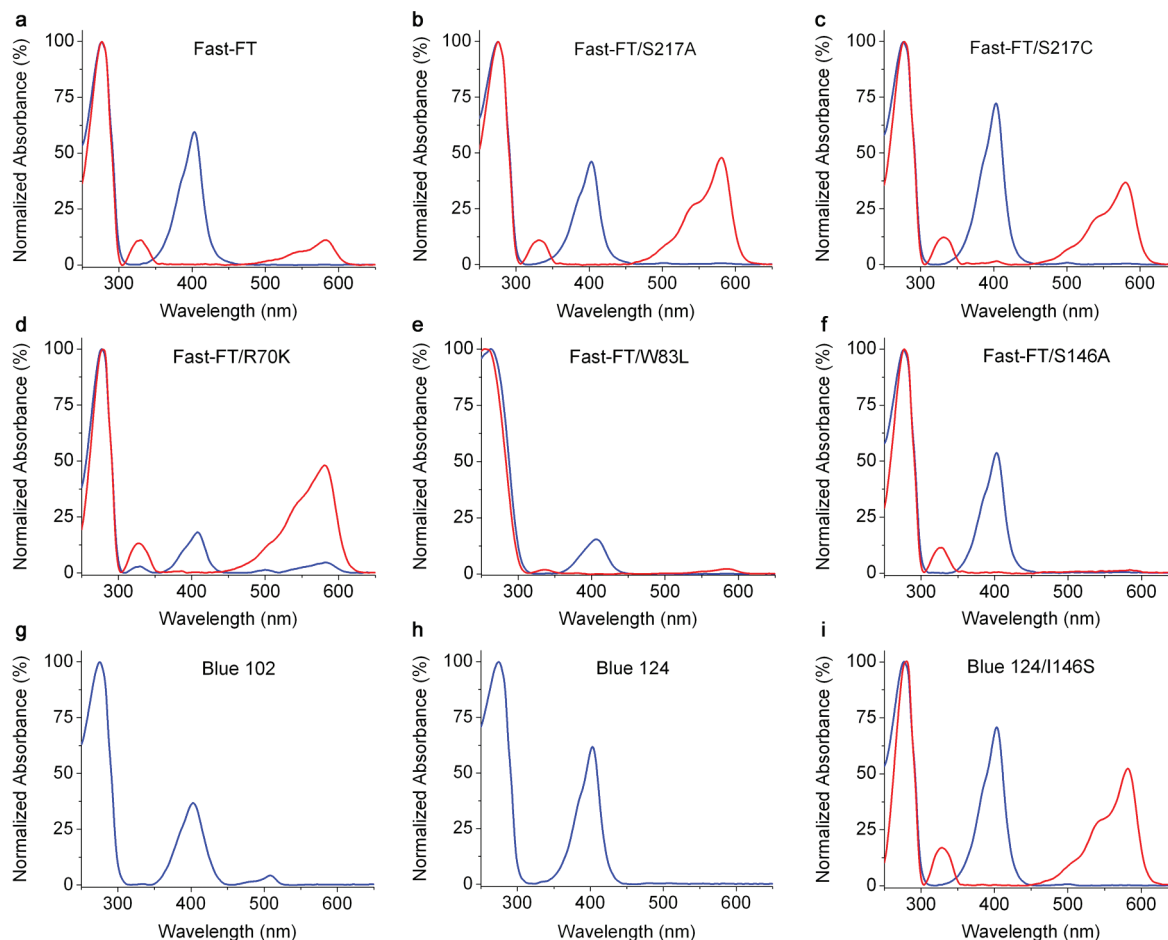


**Figure 6.** Absorbance spectra of the mutants recorded at maturation points corresponding to the maximum intensities of their blue forms (blue curves) and red forms (red curves), and normalized to the intensity of a 280 nm band.

of Lys70 to arginine in mCherry (mCherry/K70R) reduced the rate of the blue-to-red conversion 10-fold, making the mCherry/K70R variant a fluorescent timer. Purified mCherry/K70R has 13-fold lower intensity of the 583 nm absorbance band compared to that with purified Fast-FT.

Our previous studies indicated that the variants containing Trp83 generally exhibit substantially brighter blue and red fluorescence.<sup>11</sup> Indeed, a reverse Trp83Leu mutation (Fast-FT/W83L) resulted in a variant that demonstrated 5-fold decrease of both blue and red fluorescence and with greatly reduced intensities of both 403 and 583 nm absorbance bands relative to those of Fast-FT.

Mutation of Ser217 to alanine, as in the original mCherry (Fast-FT/S217A), yielded a variant with 4-fold slower development of blue form, and with roughly the same rate of red form generation as in Fast-FT. The absorbance spectra of this mutant exhibit 1.1-fold lower 320 nm and 4.3-fold higher 583 nm band intensities. Substitution of Ser217 with the isosteric cysteine (Fast-FT/S217C) yielded a timer with markedly slower formation of the blue form (9.2-fold), and with only 2.3-fold slower formation of the red form. The absorbance band intensities of the matured Fast-FT/S217C are 1.1-fold lower at 320 nm and 3.0-fold higher at 583 nm than those of Fast-FT.

The latter three mutants were aimed at probing the position 146, occupied by a serine in mCherry, Fast-FT, and other timers described in ref 11 and by isoleucine in timer precursors Blue102 and Blue124. The replacement of Ser146Ala in Fast-FT (Fast-FT/S146A) resulted in a variant with very dim red fluorescence

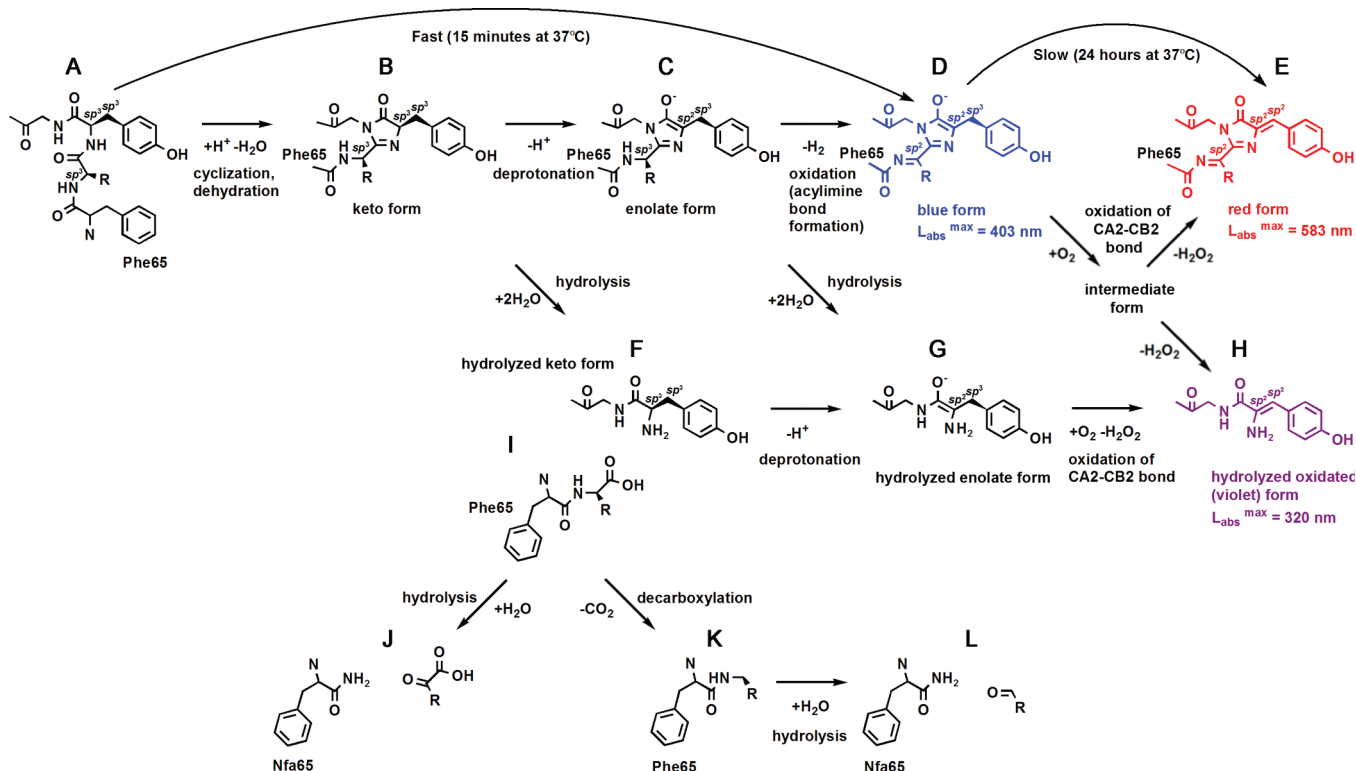
and with 8.5-fold lower intensity of the 583 nm absorbance band relative to that with Fast-FT. Substitution of Ile146Ser in Blue124 (Blue124/I146S) converted this mutant into the timer with roughly the same velocity of the formation of blue and red forms as in Fast-FT. An equivalent Ile146Ser mutation in Blue102 (Blue102/I146S) produced essentially nonfluorescent product.

#### 4. Discussion

The goals of this study were to understand the mechanism of blue-to-red conversion in FTs, to identify the residues responsible for the timing properties of Fast-FT, and to reveal their role in posttranslational chemistry of the timers. To address these questions we determined the X-ray structures of the matured Fast-FT and a timer precursor Blue102 with blue-to-red conversion blocked at the blue form, analyzed the environment of the chromophores, reverted one at a time the residues proximal to the chromophore that differ between Fast-FT and mCherry to the original mCherry sequence, and studied the spectral properties and kinetics of maturation for these mutants (Figure 6, Table 3, and Table 1s and Figure 1s of Supporting Information).

**4.1. Blue and Red Chromophores.** The structure of the timer precursor Blue102 indicates a degraded chromophore with an almost perpendicular disposition of the tyrosine and the remnant imidazolone rings and an abnormally small  $C\alpha2-C\beta2-C\gamma2$  valence angle ( $119.3^\circ$ ), suggesting  $sp^3$ -hybridization of the  $C\beta2$



Scheme 1. Posttranslational Events Taking Place in Fluorescent Timers and Their Precursors<sup>a</sup>

<sup>a</sup> Intact polypeptide (A) undergoes backbone cyclization followed by dehydration of its 5-membered ring, producing a keto intermediate (B). Deprotonation of compound (B) leads to a nonfluorescent enolate form of chromophore precursor (C). Oxidation of the N1–C $\alpha$ 1 bond to acylimine produces a blue-emitting chromophore moiety in which an active  $\pi$ -electron system is delocalized over the imidazolone and acylimine groups of the chromophore and carbonyl of Phe65 (D). (Compound D is the final product in Blue102 and Blue124 FPs.) Subsequent oxidation of the C $\alpha$ 2–C $\beta$ 2 bond occurring via an unknown intermediate engages the phenolic ring in conjugation, resulting in red chromophore (E) and compound (H). Alternatively, a chromophore precursor may undergo hydrolytic degradation which starts from the cleavage of cyclized keto (B) or enolate (C) intermediates to give products (F) and (G), respectively. Compound G is the final product of the hydrolysis pathway in Blue102 and Blue124 and is observed in the Blue102 structure. Oxidation of the C $\alpha$ 2–C $\beta$ 2 bond results in compound (H) that is the final product of hydrolytic degradation in Fast-FT. The first chromophore-forming residue (Met66 in Fast-FT and Leu66 in Blue102) (I) that becomes cleaved from the chromophore after hydrolysis undergoes further chemical transformations. In Blue102, Leu66 undergoes decarboxylation but remains attached to Phe65 (K), whereas in Fast-FT, Met66 is completely removed from the protein. Two scenarios are possible. Either (i) Met66 first undergoes decarboxylation (K) and then hydrolysis (L), or (ii) Met66 gets cleaved directly, skipping the decarboxylation step (J).

atom and consequently a single C $\alpha$ 2–C $\beta$ 2 bond (Figures 4b, 5b). This indicates that in the intact Blue102 chromophore, the tyrosine ring is excluded from conjugation, leaving the imidazolone ring and acylimine group of the chromophore, as well as the carbonyl oxygen of Phe65, to emit blue light. Fast-FT possesses an mCherry-like chromophore, with coplanar orientation of the tyrosine and imidazolone rings, and with oxidized N=C $\alpha$ 1 and C $\alpha$ 2=C $\beta$ 2 bonds (Figures 4a, 5a). The  $\pi$ -electron system is spread over the entire Fast-FT chromophore, including the tyrosine ring, resulting in red fluorescence. Our results are in full agreement with recent data on the structures of the red fluorescent protein TagRFP and of its bright blue derivative mTagBFP,<sup>32</sup> both of which contain an acylimine functionality in the chromophores. It was shown that a tyrosine ring of the blue-emitting mTagBFP chromophore is almost perpendicular to both the imidazolone and acylimine groups; mass spectrometry analysis suggests a single C $\alpha$ 2–C $\beta$ 2 bond. The red-emitting mTagRFP chromophore possesses coplanar arrangement of the phenolate, imidazolone, and acylimine groups and, according to mass spectrometry, has a double C $\alpha$ 2=C $\beta$ 2 bond.

**4.2. Blue-to-Red Conversion.** Crystal structures of Blue102 and Fast-FT clearly show that blue-to-red conversion corre-

sponds to oxidation of C $\alpha$ 2–C $\beta$ 2 bond of the chromophore. As was shown earlier for DsRed-like proteins, formation of a matured red chromophore goes via a blue-emitting intermediate.<sup>33</sup> Thus, formation of a double C $\alpha$ 2=C $\beta$ 2 bond is the last step of posttranslational modification. The mechanism of chromophore formation in FTs comprises four major steps (Scheme 1): (1) cyclization of the polypeptide backbone (B); (2) deprotonation of the cyclized intermediate resulting in enolate form (C); (3) oxidation of the N1–C $\alpha$ 1 bond to acylimine, yielding blue chromophore (D); and (4) oxidation of the C $\alpha$ 2–C $\beta$ 2 bond leading to a red chromophore (E). While DsRed goes over all the four stages in minutes, acquiring its final red-emitting form, the first three stages (A–D) take 15 min in Fast-FT, whereas the last stage (D–E), corresponding to the blue-to-red conversion, is extended to more than 24 h.<sup>11</sup>

**4.3. Residues Important for Red Chromophore Maturation and Timing Properties.** The mutants described above could be divided into three groups. Relative to the maturation steps they affect: acylimine group formation (Fast-FT/S217A and Fast-FT/S217C); oxidation of the C $\alpha$ 2–C $\beta$ 2 bond (Fast-FT/R70K, mCherry/K70R, and Fast-FT/W83L), and stabilization of the chromophore in “cis-like”/cis conformation (Fast-FT/S146A, Blue102/I146S, and Blue124/I146S).

(32) Subach, O. M.; Gundorov, I. S.; Yoshimura, M.; Subach, F. V.; Zhang, J.; Gruenwald, D.; Souslova, E. A.; Chudakov, D. M.; Verkhusha, V. V. *Chem. Biol.* **2008**, *15* (10), 1116–1124.

(33) Verkhusha, V. V.; Chudakov, D. M.; Gurskaya, N. G.; Lukyanov, S.; Lukyanov, K. A. *Chem. Biol.* **2004**, *11* (6), 845–854.

Both mutations, Fast-FT/S217A introducing Ala217 present in mCherry and Fast-FT/S217C replacing Ser217 to an isosteric cysteine, principally decrease the rate of blue chromophore formation but do not significantly affect the speed of blue-to-red conversion (Table 3, and Figure 1s of Supporting Information). Thus, the presence of Ser217 in the original Fast-FT accelerates oxidation of N1–C $\alpha$ 1 bond to acylimine, resulting in faster formation of blue chromophore. This effect is presumably due to either direct, or water-mediated interactions of Ser217 with the catalytic Glu215 located in close proximity ( $\sim$ 4 Å) to Ser217. While the side chain of Ala217 is unable to form hydrogen bonds and the thiol group of Cys217 is also a poor hydrogen bond partner, the hydroxyl group of Ser217 is capable of hydrogen bonding with the carboxylate of Glu215, facilitating proton transfer required for chromophore formation.

The mutants, Fast-FT/R70K, mCherry/K70R, and Fast-FT/W83L, demonstrate that Arg70 and Trp83 are critical for timing properties of Fast-FT. These residues affect the rate of C $\alpha$ 2–C $\beta$ 2 bond oxidation (thus controlling blue-to-red conversion) and the ratio between chromophore formation and degradation reactions. In Fast-FT, Arg70 forms a hydrogen bond with O2 of the chromophore (Figure 4). This interaction presumably induces strong polarization in the imidazolone ring, making it susceptible for hydrolysis (see below) and simultaneously slowing down the blue-to-red conversion. Lys70 in mCherry has an opposite effect—its smaller side chain forms no hydrogen bonds with the chromophore, shifts the preference toward oxidation of C $\alpha$ 2–C $\beta$ 2 bond, and accelerates this reaction. Trp83 of Fast-FT decreases the effect of Arg70 on the chromophore imidazolone ring, reducing the rate of hydrolysis and accelerating blue-to-red conversion. Indeed, Fast-FT/R70K has 10.8-fold faster blue-to-red conversion and 4.6-fold higher intensity of the 583 nm absorbance band than Fast-FT, pointing at acceleration of C $\alpha$ 2–C $\beta$ 2 oxidation and an increased yield of the red chromophore (Table 3, Figure 6, and Figure 1s of Supporting Information). mCherry/K70R has 10-fold slower C $\alpha$ 2–C $\beta$ 2 oxidation and 13-fold lower 583 nm absorption band intensity relative to mCherry, indicating a higher rate of hydrolysis. Fast-FT/W83L (this variant has an arginine at position 70) is a protein with very low 403 and 583 nm absorbance bands in which positively charged group of Arg70, uncompensated by the electron-rich indole of Trp83, rerouts posttranslational chemistry toward chromophore degradation. Apparently, it is a balanced combination of Arg70–Trp83 in Fast-FT that makes it “tick” by slowing down, but not blocking completely, the oxidation of C $\alpha$ 2–C $\beta$ 2, i.e. blue-to-red conversion.

After full maturation, Fast-FT/S146A exhibits a greatly diminished intensity of 583 nm absorbance band (Figure 6). As seen in the structure of Fast-FT, Ser146 forms a direct hydrogen bond with the p-hydroxyphenyl ring of the chromophore, stabilizing it in the *cis* configuration. Thus, Ser146 increases the extent of formation of the red form in Fast-FT by fixing the chromophore in a “*cis*-like” conformation, favorable for the oxidation process. However, the presence of Ile146 has an opposite effect. Crystal structure of Blue102 shows that Ile146 prevents the tyrosine ring of the chromophore from adopting a “*cis*-like” conformation. Substitution Ile146S in Blue124 (Blue124/I146S) results in FP with a distinct 583 nm absorbance band and the timing properties similar to those of Fast-FT, demonstrating again that a “*cis*-like” conformation of the chromophore, bringing C $\beta$ 2–H bond in appropriate position for proton abstraction, is another key factor essential for blue-

to-red conversion. A similar mutation in Blue102, which contains the chromophore triad Leu-Tyr-Gly rather than Met-Tyr-Gly seen in Blue124, mCherry,<sup>18</sup> and all timers,<sup>11</sup> gives an essentially nonfluorescent Blue102/I146S, indicating disruption of maturation pathway. Modeling studies show that the local environment is too restricted for bulky Leu66 in the intact Blue102 chromophore, which is not a case for the chromophore of Blue124, having a smaller and more flexible Met66 at this place. Leu66 forms numerous short contacts ( $\sim$ 2.0–2.5 Å) with the surrounding residues that include the catalytic Glu215, creating unfavorable interactions that might trigger chromophore decomposition. Stereochemical conflicts have been previously reported as being responsible for various chemical reactions in FPs. A few striking examples illustrating this are decarboxylation of the aspartic acid in the Asp-Tyr-Gly chromophore of zRFP574,<sup>34</sup> cyclization of lysine in the Lys-Tyr-Gly chromophore in zYFP538,<sup>14,17</sup> and cyclization of threonine in the Thr-Tyr-Gly chromophore in mOrange.<sup>18</sup>

**4.4. Hydrolysis.** The crystal structures of both Blue102 and Fast-FT indicate the presence of degraded chromophore units (Figure 5). We may conclude that the observed degradation process may have involved participation of water molecules and was apparently catalyzed by Glu215, suggesting acidic hydrolysis. The latter residue facilitates a nucleophilic attack required for both the maturation and degradation reaction pathways. This interpretation is in good agreement with a recent paper of Barondeau and colleagues on posttranslational chemistry of a GFP variant with Gly-Ser-Gly chromophore, showing that both maturation and hydrolysis reactions are catalyzed by Glu222 residue (Glu215 in Fast-FT).<sup>35</sup> The results presented here indicate that the same residues that facilitate chromophore maturation participate in its hydrolytic degradation.

The absorbance spectra of both Fast-FT/S217A and Fast-FT/S217C have higher 583 nm and slightly lower 320 nm band intensities than Fast-FT, indicating a higher yield of red chromophore and lower amount of degraded chromophore formation, respectively (Table 3, Table 1s of Supporting Information, and Figure 6). Thus, serine at position 217 not only accelerates chromophore maturation but also increases the rate of its hydrolysis. Being a member of a hydrogen-bond network surrounding the chromophore, Ser217 apparently participates in proton transfer necessary for both reactions.

Fast-FT/R70K is a mutant with 4.6-fold higher 583 nm absorbance band intensity, whereas Fast-FT/W83L is a protein with only residual quantities of blue and red chromophore species, as indicated by its very low intensities of 403 and 583 nm absorbance bands (Figure 6 and Table 1s of Supporting Information). Thus, the presence of Lys70, not making a hydrogen bond to the chromophore, reduces the rate of chromophore hydrolysis, even though this residue is positively charged. On the contrary, Arg70 of Fast-FT/W83L, hydrogen bonded with the O2 atom of the chromophore, also positively charged but uncompensated by electron-rich Trp83, increases this rate over 80%. Polarization of the imidazolone group by Arg70 makes it more susceptible to a nucleophilic attack that takes place in the first step of chromophore hydrolysis.

**4.5. Posttranslational Reactions in FTs.** Our results demonstrate that maturation and hydrolysis of FTs are essentially two competitive processes catalyzed by the same group of residues,

(34) Pletneva, N.; Pletnev, S.; Tikhonova, T.; Popov, V.; Martynov, V.; Pletnev, V. *Acta Crystallogr., Sect. D* **2006**, 62 (Pt 5), 527–532.

(35) Barondeau, D. P.; Kassmann, C. J.; Tainer, J. A.; Getzoff, E. D. *J. Am. Chem. Soc.* **2006**, 128 (14), 4685–4693.

both taking place in the course of chromophore formation. Recently, for the Gly-Ser-Gly mutant of GFP it was proposed that both maturation and hydrolysis occur through the same cyclized intermediate.<sup>35</sup> Similar to that, in FTs, hydrolysis starts from analogous cyclized product resulting from the nucleophilic attack of Gly68 nitrogen on Met66 carbonyl carbon and accompanies maturation, as a side reaction, all the way to formation of blue and red chromophores (Scheme 1). Keto (B) and enolate (C) intermediates may also undergo hydrolytic degradation. The formation of red (E) and violet (H) forms occurs synchronously, and they continue to accumulate after disappearance of the blue form (Supporting Information, Figure 1s), suggesting that they both originate from the common intermediate formed from the blue chromophore (Scheme 1). The presence of such an intermediate was demonstrated earlier by kinetic study for Fast-FT.<sup>11</sup> The formation of the violet and red forms occurs only in the presence of oxygen, suggesting that the intermediate form may represent an unstable peroxy adduct. These conclusions are in agreement with a recent proposal suggesting that oxidation of the C $\alpha$ 2–C $\beta$ 2 bond in GFP is an oxygen-dependent, multistage process utilizing a radical-based mechanism.<sup>36</sup> The developed chromophores apparently become much more resistant to hydrolysis; the matured FTs are very stable and retain virtually unchanged spectral characteristics even after a few months storage at 4 °C. The stability of FTs, however, greatly depends on temperature; as is clearly seen in X-ray structures obtained for crystals grown at ambient temperature, the red and blue chromophore moieties undergo partial or complete hydrolytic degradation after 2–3 weeks.

## 5. Summary

Maturation of FT chromophores proceeds through a blue-emitting intermediate that contains a single C $\alpha$ 2–C $\beta$ 2 bond. Oxidation of this bond is the last step of posttranslational

modification that results in a red chromophore. Whereas the nature of the residue at position 217 alters the speed of blue chromophore formation, the residues at positions 70 and 83 determine the rate of blue-to-red conversion. Serine at position 217 markedly accelerates formation of blue chromophore but does not affect much the speed of blue-to-red conversion. On the other hand, lysine at position 70 or leucine at position 83 has little effect on the kinetics of blue chromophore formation but greatly accelerates formation of red chromophore. Combination of Arg70 and Trp83 is a key factor slowing down blue-to-red conversion and therefore introducing timing properties in Fast-FT. Oxidation of the C $\alpha$ 2–C $\beta$ 2 bond is dependent on “*cis*-like” orientation of the chromophore. Therefore, in timers Ser146, stabilizing “*cis*-like” orientation of the moiety, is another residue crucial for blue-to-red conversion. In FTs, chromophore maturation and hydrolysis are competitive processes that are driven by the same group of residues. Taken together, these results suggest how to alter the kinetics of a particular stage of posttranslational reactions, providing a basis for the development of novel biomarkers with time-resolved properties.

**Acknowledgment.** Diffraction data were collected at the SER-CAT ID22 beamline at the Advanced Photon Source, Argonne National Laboratory. Use of the Advanced Photon Source was supported by the U.S. Department of Energy, Office of Science, Office of Basic Energy Sciences, under Contract No. W-31-109-Eng-38. This project has been funded in part with Federal funds from the National Cancer Institute, National Institutes of Health (NIH) Contract No. HHSN261200800001E, the Intramural Research Program of the NIH, National Cancer Institute, Center for Cancer Research, and by the NIH Grant GM073913 to V.V.V. The content of this publication does not necessarily reflect the views or policies of the Department of Health and Human Services, nor does the mention of trade names, commercial products or organizations imply endorsement by the U.S. Government.

**Supporting Information Available:** This material is available free of charge via the Internet at <http://pubs.acs.org>.

JA908418R

(36) Barondeau, D. P.; Kassmann, C. J.; Tainer, J. A.; Getzoff, E. D. *J. Am. Chem. Soc.* **2007**, *129* (11), 3118–3126.

(37) Pace, C. N.; Vajdos, F.; Fee, L.; Grimsley, G.; Gray, T. *Protein Sci.* **1995**, *4* (11), 2411–2423.